

Characterizing the Association Between Nighttime Crashes and Retroreflectivity of Edgelines and Centerlines on Michigan Rural Two-Lane Highways

**Corresponding Author*

1) Raul E. Avelar, Ph.D.
Texas A&M Transportation Institute
The Texas A&M University System
3135 TAMU
College Station, TX 77843
Phone: 979-862-1651
e-mail: r-avelar@tamu.edu

2) Paul J. Carlson, Ph.D., P.E.
Texas A&M Transportation Institute
The Texas A&M University System
3135 TAMU
College Station, TX 77843
Phone: 979-847-9272
e-mail: paul-carlson@tamu.edu

Word Count: 5280 words + (250 x 8 Tables and Figures) = 7280 total
Re-Submitted on: March 15, 2014
93rd Annual Meeting of the Transportation Research Record

ABSTRACT

Retroreflectivity of longitudinal pavement markings is expected to improve safety on rural highways. However, the few available research reports focused on the relationship between retroreflectivity and safety have found mixed results. This paper provides new insights into such a relationship by using Generalized Linear Mixed-Effects Models (GLMM). Using this tool, the research team developed and analyzed a database of rural two-lane roads in Michigan, including night crashes, roadway characteristics, and retroreflectivity of pavement markings. The analysis used crash data from years 2003 through 2008, for select types of nighttime crashes. The analysis found a statistical association between pavement marking retroreflectivity and nighttime safety. A significant statistical interaction between white edge and yellow center line retroreflectivity indicates that these variables perform inter-dependently.

In general, sites with higher retroreflectivity were found to associate with fewer crashes than sites with lower retroreflectivity for both types of markings. This research also found that sites with low center line retroreflectivity (compared to edge line retroreflectivity of the same road) were associated with more crashes.

Keywords:

Safety modeling, retroreflectivity, pavement markings, night crashes

INTRODUCTION

This research was conducted as a follow-up to a prior effort that was initiated to determine whether a correlation between pavement marking retroreflectivity and safety could be established (1). The earlier findings lend support to the positive safety effects of maintaining retroreflectivity of pavement markings, particularly on rural two-lane highways. The purpose of this paper is to offer additional insights on the combined nighttime associations of edge line and center line pavement marking retroreflectivity levels to nighttime crashes in two-lane rural highways.

BACKGROUND

On April 22, 2010, the Federal Highway Administration (FHWA) published in the Federal Register a Notice of Proposed Amendment (NPA) to amend the Manual on Uniform Traffic Control Devices (MUTCD). This amendment included standards, guidance, options, and supporting information related to maintaining minimum levels of retroreflectivity for pavement markings. The NPA was issued in response to section 406 of the Department of Transportation and Related Agencies Appropriations Act, 1993 (Pub. L. 102-388; October 6, 1992). Section 406 of the Act directed the Secretary of Transportation to “*revise the Manual on Uniform Traffic Control Devices to include – (a) a standard for a minimum level of retroreflectivity that must be maintained for pavement markings and signs, which shall apply to all roads open to public travel.*” Improving safety throughout the transportation network is the primary goal of the Department of Transportation. The FHWA’s intent about minimum retroreflectivity levels in the MUTCD is to advance safety by meeting the nighttime visibility needs of the driver on our Nation’s roads. The comment period for the NPA related to pavement marking retroreflectivity closed on August 20, 2010. The FHWA received 105 letters submitted to the docket containing about 700 individual comments on the NPA. The FHWA has not yet responded to the comments received.

To support the NPA, the FHWA commissioned research to develop recommended minimum pavement marking levels based on the needs of nighttime drivers (2). While there is a general belief among the engineering community in a link between retroreflectivity and nighttime safety, few studies have tried to quantify the relationship.

It should be pointed out that the FHWA minimum retroreflectivity levels proposed in the NPA were developed based on the visibility needs of nighttime drivers. This is different from safety-derived minimum retroreflectivity levels, which is the focus of the work described in this paper.

LITERATURE REVIEW

In a paper presented at the TRB Annual Meeting in 2013, the findings from four pertinent studies were critiqued and summarized, demonstrating mixed results (1). Two of the studies concluded that there is no relationship (3; 4), but both studies appear to have important limitations. One study in New Zealand compared crash rates in a before-after fashion, to take advantage of a new policy that established a minimum of 70 mcd/m²/lx for pavement markings in 1997. This study relied on the assumption of brighter markings in the after period. However, the analysis did not control for delineators or RRPM, which have been found safety influential in other research (5). The other study used a large dataset from

California in combination with sophisticated statistical techniques. They concluded that the safety association of longitudinal pavement markings is approximately zero. However, this study has two important limitations: retroreflectivity was modeled instead of measured from the field, and the safety analysis incorporated the modeled retroreflectivity data as discrete bins that were determined in a linear fashion. Other works have shown that retroreflectivity is described logarithmically better than linearly (6; 7; 8).

The other two studies point to some possible relationships with statistical significance but their findings suggest small and inconsistent safety associations (9; 10). The most recent study provides the strongest link between pavement marking retroreflectivity and safety, albeit lacking the consistency to establish crash modification factors or make comparisons to other low-cost safety countermeasures (1).

Table 3A-1 of publication No. FHWA-SA-10-015 (11) proposes minimum retroreflectivity levels for both white and yellow longitudinal pavement markings equally (this document is still in draft form). Regarding two lane roads with center line markings only, this table recommends a minimum of 250 mcd/m²/lux for speed limits larger than or equal to 55 mph, 100 mcd/m²/lux for speed limits ranging from 30 to 50 mph, and no minimum for roads with speed limits at 30 mph or below.

DATA COLLECTION AND PROCESSING

The research team compiled data from various sources in the state of Michigan to assemble a database adequate for the objectives of this research. Next, a brief description of each of the data sources is provided. Further data characteristics can be found at Carlson et.al (1), since this work also utilized most of these data sources.

Retroreflectivity Database

The state of Michigan was selected because of their systematic documentation of retroreflectivity values in their roadway network at various points in time. Because of the need to plow snow during a large portion of the year, the Michigan DOT restripes approximately 85% of their roads on a yearly basis. Although the Michigan DOT collects retroreflectivity readings throughout the year, most of the recorded values for retroreflectivity are taken in the second half of the summer.

Only rural two-lane roads are analyzed in this paper. Therefore, the types of pavement markings of interest are white edge and yellow center lines only. For reasons similar to those of Carlson et.al (1), the research team opted to exclude the summer and winter months from the analysis: The first period because most of the restriping occurs during the summer and the second because winter conditions in Michigan are believed to be associated with additional safety concerns, such as rain and snow. Only actual retroreflectivity readings were used in the statistical analysis.

Roadway Database

Uniform road Segments were determined by combining the Michigan retroreflectivity database with the roadway database. This database contains traffic volumes, lane width, roadway width, and shoulder width, among other road characteristics. No information about the horizontal alignment was available from database.

Horizontal Alignment Database

Additional data on horizontal alignment were solicited from the Highway Safety Information System (HSIS). The most recent year available in the data provided by HSIS was 1997. Regardless, the research team considered that these data were adequate to discriminate tangent and curve sections effectively, since drastic changes in horizontal alignment are expensive and are thus rare.

Crash Database

The assembling of the database, containing at this point retroreflectivity data, road characteristics and horizontal alignment, was then merged with the crash database from the Michigan DOT. Crash data for the period between 2003 and 2008 were incorporated from this source to the final database.

The field “crash type” in the Michigan database was used to exclude angle and rear-end collisions as these crashes are the less likely to be influenced by retroreflectivity of the pavement markings. The reduced pool of crashes then included single vehicle, sideswipe and run-off-road crashes only. A final filter was applied to include only crashes that occurred at nighttime.

Overall Database for Analysis

The research team performed further partition of long segments before proceeding with the analysis. Those segments larger than 3 miles were subdivided into 3 miles or less. After removing segments with additional passing or turning lanes, segments with wide or raised median types, and segments identified as located in urban areas, there were 1955 valid data points representing 513 2-lane tangent segments.

TABLE 1 shows summary statistics of the final filtered tangent dataset. Jointly, there are 1024 night crashes recorded during the analysis period at the 513 segments. The total length of these segments is 860 miles.

Horizontal Curve Data

The research team made an effort to build a dataset of horizontal curve segments. Unfortunately, only 175 valid data points at curvilinear segments were available after the filtering procedure was followed as previously explained. These data points only represent 21 segments with at least one curve, having a combined length of 12 miles. Because of this limited dataset, the curvilinear segments were used to assess the safety association of retroreflectivity preliminarily only.

MODELING SAFETY OF RETROREFLECTIVITY AT TANGENT SITES

The challenge of linking retroreflectivity to crashes is their different variation periods: retroreflectivity varies considerably throughout the restriping cycle (which spans a year in Michigan); in contrast, crashes are rare events, so it is very difficult to observe trends in such short a period as one year. Therefore, the common practice of aggregating crashes in multiple years is problematic when dealing with retroreflectivity data.

The research team chose Generalized Linear Mixed-Effects Models (GLMMs) for the statistical analysis. The use of GLMMs allows one to model crashes from multiple periods but from the same spatial units without the need to aggregate data. GLMMs explicitly define

random effects to account for various types of commonalities among data points as an explicit correlation structure (12). A Negative Binomial distribution was selected to model the distribution of the response variable (i.e. nighttime crashes). Such a model links the natural logarithm of the response variable to a linear combination of the explanatory variables and the random effects. Formally,

$$\begin{aligned} \text{Night. Crashes} &\sim \text{NB}(\mu, \theta) \\ \ln(\mu|X, \alpha) &= X' \cdot \beta + \sum \alpha_i \end{aligned}$$

Where,

<i>Night. Crashes</i>	=	Nighttime crashes in the sample of roads;
<i>NB(.,.)</i>	=	Negative binomial distribution;
μ	=	Expected number of nighttime crashes;
θ	=	Dispersion parameter in the negative binomial distribution;
<i>X</i>	=	Vector of fixed effects;
β	=	Vector of coefficients; and
α_i	=	i-th random effect.

All statistical analyses were performed using open source statistical software (13; 14; 15; 16).

The general modeling process utilized stepwise selection with approximately 50 candidate variables available from the assembled dataset, such as lane width, roadway width, shoulder width, percentage of commuting traffic, median width, type of shoulder, and other variables. This process was divided in two stages: first, developing the best available model that does not account for retroreflectivity (i.e. the base model); and second, expanding the base model while allowing retroreflectivity variables to enter the pool of candidate variables.

Model Selection for Tangent Segments

In the first stage of model selection, Annual Average Daily Traffic (AADT), Segment Length, and Speed Limit were selected as the minimum set of explanatory variables (i.e. the fixed effects). Site ID and Route ID were accounted for as random effects in the correlation structure. Random effects for Year and Period (April-May and Sept-Oct) were initially considered but later dropped based on the Akaike Information Criterion (AIC). The model parameters were determined by Maximum Likelihood.

TABLE 2 shows the proposed model at the leftmost column along with prior versions connecting it from the base model, the rightmost column. The relatively large NB2 theta coefficients indicate that all the models are mildly disperse above the Poisson distribution. The ICC indicates the degree of similarity among data points within each level.

It is worth noting that the coefficient for Ln(Segment Length) is statistically equivalent to one across all models. Therefore, similar results may be obtained if segment length were treated as an offset instead of an estimated coefficient. Coefficients of variables unrelated to retroreflectivity show little variability among models, a fact suggesting that such variables are relatively independent of the retroreflectivity.

The random effects are also stable across the table. The Intraclass Correlation Coefficients (ICC) are also stable.

The first inclusion of retroreflectivity in the White-Yellow Retro Model (fourth column in TABLE 2) shows that only white edge is barely statistically significant with a positive sign. This is contrary to expectation. In contrast, the coefficient for the retroreflectivity of yellow center line is negative but statistically insignificant. The authors suspect the straight interpretation of these coefficients because the spatially-weighted correlation between the white and yellow retroreflectivities is quite high: +0.41. Comparatively, this correlation almost doubles the correlation between the response variable (Nighttime crashes) and its closest related covariate, segment length. Under such circumstances, multicollinearity may be inflating the retroreflectivity standard errors, which very likely explains the lack of significance of yellow centerline retroreflectivity.

The research team found a mild improvement in the goodness of fit when accounting for an interaction between the retroreflectivity variables, shown as W.Y Interaction model in the table. This model requires interpreting the effects of the two retroreflectivity variables jointly. This circumstance is inescapable, not only because of the high correlation between retroreflectivity values, but also because it is plausible that both retroreflectivity variables have a joint (not an individual) bearing on safety. The research team elected to refine this model further continuing with the analysis. The proposed model embodies such refinements, which will be explained in the next section.

Model refinement

There are two further refinements to the interaction model that led to the proposed model: (1) coefficient estimation on rotated axes, and (2) definition of a reference level.

In general, the formulation of a bilinear polynomial produces a family of response surfaces capable to accommodate a wide range of variability. However, the resulting surfaces are always bounded to rises and drops such that the gradients converge to lines at 45° with the covariate axes, white and yellow retroreflectivities in this case. Axis rotation is a potential remedy for this constraint. This technique increases the potential of detecting surfaces that may be oriented otherwise. Indeed, the research team found a significantly better fit (given the same degrees of freedom) when repeating the model estimation at 45 degrees of clockwise rotation. Equation 1 shows the general formulation for the rotation of orthogonal axes:

Equation 1 Axis rotation of white and yellow retroreflectivity levels.

$$[W', Y'] = [W, Y] \times \begin{bmatrix} \cos(\alpha) & -\sin(\alpha) \\ \sin(\alpha) & \cos(\alpha) \end{bmatrix}$$

Where,

- W = A column vector with the white edge values;
- Y = A column vector with the corresponding yellow center values;
- W' = A column vector with corresponding values on the rotated white axis;
- Y' = A column vector with corresponding values on the rotated yellow axis; and
- α = An angle of rotation.

It is important to notice that for $\alpha = -45^\circ$:

$$W' = 0.7071 \times W - 0.7071 \times Y; \text{ and}$$

$$Y' = 0.7071 \times W + 0.7071 \times Y.$$

For simplicity, the authors preferred the linear combinations (W-Y) and (W+Y) instead of using such rotated coordinates. The rotated variables are simply the linear combinations scaled by a factor of 0.7071. These linear combinations can be interpreted on their relation to the measured retroreflectivity of white and yellow lines more easily, as will be noted later in this paper.

The second refinement that allowed the research team to arrive at the proposed model consisted of a calibration of the bilinear polynomial formulation to a reference level. This calibration is such that the polynomial yields a value of 1.0 at certain reference values for the covariates. Such a calibrated polynomial can be interpreted directly as Crash Modification Function (CMF), per the methodologies of the Highway Safety Manual (HSM). The proposed model, therefore, accounts for the safety of retroreflectivity in the following general form:

Equation 2 General formulation for a retroreflectivity Crash Modification Factor at nighttime.

$$CMF = \exp[\beta_{\Sigma} \times (\Sigma Retros - ref_{\Sigma}) + \beta_{\Delta} \times (\Delta Retros - ref_{\Delta}) + \beta_{\Sigma,\Delta} \times (\Sigma Retros - ref_{\Sigma}) \times (\Delta Retros - ref_{\Delta})]$$

Where:

CMF	=	Crash Modification Function associated with retroreflectivity levels;
$\Sigma Retros$	=	Sum of white edge line and yellow center line retroreflectivities;
$\Delta Retros$	=	Difference between white edge line and yellow center line retroreflectivities;
$ref_{\Sigma}, ref_{\Delta}$	=	Reference level for $\Sigma Retros$ and $\Delta Retros$ respectively; and
$\beta_{\Sigma}, \beta_{\Delta}, \beta_{\Sigma,\Delta}$	=	Coefficient estimates, obtained via GLMM.

NIGHTTIME CRASH MODIFICATION FUNCTION FOR RETROREFLECTIVITY

For the CMF reference levels, the research team elected values of $ref_{\Sigma} = 325 \text{ mcd/m}^2/\text{lx}$ and $ref_{\Delta} = 80 \text{ mcd/m}^2/\text{lx}$ because about 98% of all the retroreflectivity data exceeds these values, so the CMF reference is at the low percentiles of the sample at hand.

When using such reference levels, the CMF takes the specific form:

Equation 3 Crash Modification Factor for retroreflectivity at nighttime.

$$CMF = 0.3680 \times \exp[1.945 \times 10^{-3} \times (\Sigma Retros) + 1.038 \times 10^{-2} \times (\Delta Retros) - 1.780 \times 10^{-5} \times (\Sigma Retros) \times (\Delta Retros)]$$

FIGURE 1 shows a scatter plot of the original retroreflectivity data overlapped by a contour map of the CMF in the 2-dimensional space defined by the sum and the delta of the retroreflectivity values. In addition, the figure shows ellipses containing approximately 50% and 95% of the data.

The safety association of retroreflectivity can be described as a function of two factors: the sum of white and yellow retroreflectivity levels, and the difference between white and yellow retroreflectivities. The first factor can be understood as a measure of total brightness; the second can be viewed as a measure of how much less bright the yellow center line is compared to the white edge line.

Imagining horizontal lines in FIGURE 1 at various levels of Delta and examining the trends, one can see that safety improves in proportion to the sum of retroreflectivities. This improvement is rapid and clear at higher deltas but less clearly at lower deltas. In contrast, when imagining vertical lines at various levels of sum and examining the trends, one can see that safety deteriorates in proportion to how big the difference between retroreflectivities is. This trend is more rapid and clear at lower sums of retroreflectivities, but somehow equivocal at higher values for the sum of retroreflectivities.

The previous observations can be better grasped by looking at the families of curves that result from holding one of the variables in the CMF constant while allowing the other to vary (i.e. sum and delta of retroreflectivities). These are the exponential curves shown in FIGURE 2 and FIGURE 3. Dashed lines represent cases that are statistically equivalent to a flat line at 1.0. To determine this equivalency, a significance level of 0.05 was chosen from a statistical test on the exponent of the Partial CMF on one variable and fixed at a particular value of the other variable (17).

It is clear from FIGURE 2 and FIGURE 3 that these are competing factors, with their respective influence being predominant at opposite conditions. On the one hand, the improving safety trend associated with increasing sum of retroreflectivities is statistically significant when the deltas are high. On the other hand, the decline in safety associated with increasing deltas is statistically significant when the sum of retroreflectivities is small.

Yearly Variation of the CMF at a Hypothesized Location

To illustrate the safety implications of the retroreflectivity safety model, the research team reviewed the variation of the CMF at a hypothetical site that is annually restriped, as is the case in Michigan. It should be noted that this example includes months that were not part of the analysis, yet the exercise is useful to depict how safety should vary, as of the model, when the retroreflective material degrades over a year.

It is reasonable to presume large values for both white and yellow lines immediately after restriping, say, (450W, 250Y). It is also reasonable to suppose that these values fall together during a year as the retroreflective material deteriorates. To project the deterioration of the material in this example the research team assumed a logarithmic decay, similar to the degradation curves fitted by Kopf (8). From the available data, the rate between the two periods in the dataset was determined to be 0.9307, or 6.93% monthly decay for white edge and 0.9103 or 8.97% monthly decay for yellow centerlines.

FIGURE 4 shows a yearly trace of the projected deterioration of white and yellow lines. This figure also shows the safety factor values corresponding to the hypothesized pairs of white and yellow values.

According to FIGURE 4, the safety of the site would deteriorate as retroreflectivity decays. This safety deterioration is indicated by the safety factor line rising from 0.947 up to a value

of 1.160 (i.e. a 16% increase in crashes) just before restriping is due again. However, it should be noted that the maximum value the CMF reaches is 1.255 in January, from where it falls to 1.160 in July, even when retroreflectivity of both yellow and white keep falling during this period.

FIGURE 2 and FIGURE 3 should help explaining this counter intuitive behavior: At the beginning of the exercise, the large sum of retroreflectivities controls and the CMF is low, despite the largest delta. Most of the safety detriment (i.e. CMF increase) is associated with a rapid fall of the sum of retroreflectivities overcoming the impact of a slower fall of the delta, as both retroreflectivities decay. The CMF increasing trend flattens as the sum of retroreflectivities become smaller and even reverses as narrower deltas start to become the dominant feature of the joint decay of retroreflectivities.

FIGURE 4 also shows 95% confidence intervals for the CMF (using the standard errors of the GLMM estimates). These intervals are provided so to get a sense of how the variability associated with the CMF estimates impact the certainty associated with the effect at different levels of the restriping cycle. From these confidence intervals, one can see that the CMF clearly exceeds 1.0 as the decay of white retro reaches 314 mcd/m²/lx and yellow falls to 158 mcd/m²/lx. The CMF remains larger than one as both retroreflectivities continue to decay.

Sensitivity Analysis of the retroreflectivity CMF

This evaluation was based on the statistical significance of the CMF, which is a function of the sample size and the range of retroreflectivity values represented in the database. This evaluation focuses on identifying a region where the CMF magnitude is clearly in excess of 1.0.

The procedure consisted in obtaining the standard error of the CMF for every available data point, then mapping the statistical significance of a test on the null hypothesis that the joint effect be 1.0 at most.

FIGURE 5 shows the result of this evaluation. The figure indicates that the joint effect is indistinguishable from 1.0 for most of the dataset. There is, however, a region where the CMF clearly exceeds 1.0. This region is the majority of sites with deltas exceeding 100 mcd/m²/lx and with sums not exceeding 530 mcd/m²/lx. For this subset of sites, the evidence of more crashes becomes more compelling as deltas increase and sums decrease.

FIGURE 6 shows the mapping of the statistical significance of the CMF similar to FIGURE 5 but including with two additional features: the coordinates are White and Yellow retroreflectivities, instead of their sum and delta; and the average CMF within each zone of statistical significance.

In the zone where the CMF is larger than one (with a statistical significance of 0.05 or smaller), this figure shows that the yellow retroreflectivity level is a clear indicator of high CMF values: all these sites have yellow retroreflectivity smaller than 165 mcd/m²/lx. There is an average expectation of 20% more crashes for the sites with higher yellow retroreflectivity in this region, but it can be up to 27% more crashes for the sites with lower yellow retroreflectivity.

SAFETY OF PAVEMENT MARKING RETROREFLECTIVITY AT CURVE SITES

An additional safety analysis of retroreflectivity at curve segments was initially intended for this research effort. However, sample size was a serious limitation. The research team could

identify only 64 single curves in the dataset, which is a sample size barely suitable to fit up to two parameters using generalized linear models. Notwithstanding, the research team tested how well the coefficients available from the analysis of tangent sections perform in the curve data at hand. This evaluation found the contribution of the CMF significant only in the case of single curves. After accounting for radius of curvature, this statistical evaluation showed that the CMF requires a calibration factor of 1.72 (Standard error of 0.671) at curves sites. More research is needed to study the safety implications of retroreflectivity at curve sites.

SUMMARY OF FINDINGS AND CONCLUSIONS

A database of crashes, roadway characteristics, horizontal alignment, and retroreflectivity records was assembled using data available from state-maintained roads in Michigan. The analysis presented in this paper uses GLMMs to deal with time-resolution and data structure correlations.

Results indicate that, in general, retroreflectivity of pavement markings at two way rural roads in Michigan tend to relate to safety. In particular, this analysis found that there is a joint association between retroreflectivity of both white edge and yellow center lines to nighttime crashes at tangent sections. This relationship is captured by two linear combinations of white and yellow retroreflectivity: the sum of retroreflectivity values, which represents how bright both pavement markings are in general; and the difference of retroreflectivity values, which represents how much less bright the yellow center line is in comparison to the white edge line. The sum of retroreflectivities was found to relate to nighttime crashes in inverse proportion. Conversely, the delta of retroreflectivities was found to relate to night crash frequency in direct proportion. In other words, sites with brighter pavement markings tend to have fewer nighttime crashes, but that trend is weaker at sites with bigger brightness gaps between yellow center lines and white edge lines.

The research team performed this estimation by use of a CMF emerging from the statistical analysis, given the range of retroreflectivity values in the Michigan dataset. This evaluation quantified how sites with the brightest pavement markings and relatively brighter yellow markings (i.e. sites with large sums and small deltas) are characterized by fewer crashes than otherwise. A sensitivity analysis of these trends did not find much variation in safety for most of the range in the retroreflectivity dataset. However, there is statistical evidence of an increased risk of nighttime crashes for sites with yellow markings having retroreflectivity levels less than $165 \text{ mcd/m}^2/\text{lx}$. Such risk increases in inverse proportion to the total brightness (i.e. sum of white and yellow retroreflectivities) and direct proportion to how big the brightness gap of yellow line is with respect to white line (i.e. increasing deltas).

The authors also evaluated safety of curve segments as it relates to the retroreflectivity values. Unfortunately, only a preliminary assessment was possible, given the small dataset for curve sites. When comparing the CMF from tangent segments to single curve locations, the results showed that retroreflectivity safety behaves similarly at those locations, after accounting for radius of curvature. However, the evaluation estimated an adjusting factor of 1.724, which indicates that pavement marking retroreflectivity may be even more relevant at curves than at tangent sections in terms of safety. However, this finding is not robust, given that it is based on the data from 64 sites only. No evidence was found of similar concomitance of the tangent CMF and sites with more than one curve. The research team recognizes the need of future research considering locations with increased geometric complexity in general, but particularly at sites with horizontal curvature.

ACKNOWLEDGEMENTS

The authors would like to thank the personnel from the Highway Safety Information System for providing the horizontal alignment data necessary to perform this research. The authors would also like to thank the Michigan DOT for sharing their data. Finally, the authors would like to thank Dong Hun Kang of TTI for his assistance with the construction of the databases.

REFERENCES

1. Carlson, Paul J., E. S. Park, and D.H. Kang. An Investigation of Longitudinal Pavement Marking Retroreflectivity and Safety. Washington DC: *Transportation Research Record, the Journal of the Transportation Research Board*. Transportation Research Board of the National Academies. Washington DC, 2013, (pending publication).
2. Debaillon, Chris, P. Carlson; Y. He, T. Schnell, and F. Aktan. *Updates to Research on Recommended Minimum Levels for Pavement Marking Retroreflectivity to Meet Driver Night Visibility Needs*. McLean, VA: Federal Highway Administration, 2007. FHWA-HRT-07-059.
3. Dravitzki, V. K., S.M. Wilkie, and T.J. Lester. *The Safety Benefits of Brigher Roadmarkings*. Wellington, New Zealand : Land Transport, 2006.
4. Bahar, J. M., M. Masliah, T. Erwin, E. Tan, and E. Hauer. *Pavement Marking Materials and Markers: Real-World Relationship between Retroreflectivity and Safety over Time*. NCHRP Web-Only Document 92. onlinepubs.trb.org. [Online] April 2006. http://onlinepubs.trb.org/onlinepubs/nchrp/nchrp_webdoc_92.pdf. [Accessed on: November 2013.]
5. Molino, J. A.; K. S. Opiela, C.K. Andersen, and M. J. Moyer. Relative Luminance of Retroreflective Raised Pavement Markers and Pavement Marking Stripes on Simulated Rural Two-Lane Roads. *Transportation Research Record: Journal of the Transportation Research Board*. No. 1844, Transportation Research Board of the National Academies. Washington DC, 2003, pp. 45-51.
6. Aktan, F. and T. Schnell. Performance Evaluation of Pavement Markings Under Dry, Wet, and Rainy Conditions in the Field. *Transportation Research Record: Journal of the Transportation Research Board*. No. 1877. Transportation Research Board of the National Academies. Washington DC, 2004, pp. 38-49.
7. Finley, M. D., P.J. Carlson, N. D. Trout, and D. L. Jasek. *Sign and Pavement Marking Visibility from the Perspective of Commercial Vehicle Drivers*. Texas Department of Transportation, Austin, TX , 2002. FHWA/TX-03/4269-1.
8. Kopf, J. *Reflectivity of Pavement Markings: Analysis of Retroreflectivity Degradation Curves*. Washington State Department of Transportation. Olympia, WA , 2004. WA-RD 592.1.

9. Donnell, E. T. and S. Sathyanarayanan. *Exploring the Statistical Association between Pavement Markings Retroreflectivity and Traffic Crash Frequency on Two- and Multilane Highways in North Carolina*. Pennsylvania State University. University Park, PA, 2007.
10. Smadi, O., N. R. Hawkins, R. R. Souleyrette, and D. Ormand. Analysis of Safety Effectiveness of Pavement Marking Retroreflectivity. *Transportation Research Board Annual Meeting*, Washington DC, 2008.
11. FHWA. Summary of the MUTCD Pavement Marking Retroreflectivity Standard. *FHWA Safety*. [Online] April 2010.
http://safety.fhwa.dot.gov/roadway_dept/night_visib/fhwasa10015/. [Accessed: 4 November 2013.]. FHWA-SA-10-015.
12. Pinheiro, J. and D. M. Bates. *Mixed-Effects Models in S and S-PLUS*. New York : Springer, 2000. ISBN 0-387-98857-9.
13. The R Development Core Team. *R: A Language and Environment for Statistical Computing*. [Online] R Foundation for Statistical Computing, Vienna, Austria, 2013. Version 2.10.1 (2009-12-14). <http://www.R-project.org>. ISBN 3-900051-07-0.
14. Venables, W. N. and B. D. Ripley. *Modern Applied Statistics with S. Fourth Edition*. Springer, New York, 2002. ISBN 0-387-95457-0.
15. Fox, J. and S. Weisberg. *An {R} Companion to Applied Regression, Second Edition*. Sage. Thousand Oaks, CA, 2011.
16. Bates, D., M. Maechler, and B. Bolker. *lme4: Linear mixed-effects models using Eigen and S4*. R package version 0.99999911-0/r1788. [Online] <http://R-Forge.R-project.org/projects/lme4/>.
17. Wackerly, D., W. Mendenhall III, and R.L. Scheaffer. *Mathematical Statistics with Applications. 7th Edition*. Thomson. Toronto, Canada, 2008.

LIST OF TABLES AND FIGURES

TABLE 1 Summary Statistics for Tangent Sections

TABLE 2 Retroreflectivity Safety Models

FIGURE 1 Contour plot for the safety factor of sum and delta of retroreflectivities of pavement markings.

FIGURE 2 Marginal CMFs on the sum of retroreflectivities.

FIGURE 3 Marginal CMFs on the delta of retroreflectivities.

FIGURE 4 Yearly cycle trace of retroreflectivity and its safety factor for a hypothesized site.

FIGURE 5 Statistical significance of $H_0: CMF > 1.0$.

FIGURE 6 Average CMF by zone of Statistical Significance.

TABLE 1 Summary Statistics for Tangent Sections

Variable	Mean	Std.Dev.	Min	Max	Total
Night Crashes (no.)	0.52	0.96	0	7	1,024
Segment Length (miles)	2.05	1.06	0.03	3.00	860
Lane Width (ft)	11.55	0.52	10.00	12.00	
Speed Limit (mph)	54.49	3.13	25.00	55.00	
AADT (vehicles per day)	3,341.75	2,625.35	194	22,327	
White Edge Retro (mcd/m ² /lx)	321.44	61.21	88	487	
Yellow Center Retro (mcd/m ² /lx)	178.19	30.86	61.00	294.00	

TABLE 2 Retroreflectivity Safety Models

	Proposed Model	W.Y Interaction Model	W.Y Retro Model	Base Model
Term	Estimate (Std.Err.)	Estimate (Std.Err.)	Estimate (Std.Err.)	Estimate (Std.Err.)
(Intercept)	-9.692 (1.625)***	-10.96 (1.811)***	-9.719 (1.647)***	-9.531 (1.613)***
Ln(AADT)	6.052×10^{-1} (7.112×10^{-2})***	6.019×10^{-1} (7.125×10^{-2})***	6.078×10^{-1} (7.153×10^{-2})***	5.939×10^{-1} (7.062×10^{-2})***
Ln(Segment Length)	9.047×10^{-1} (6.666×10^{-2})***	9.043×10^{-1} (6.692×10^{-2})***	9.077×10^{-1} (6.703×10^{-2})***	9.066×10^{-1} (6.705×10^{-2})***
Speed Limit	5.885×10^{-2} (2.718×10^{-2})*	5.894×10^{-2} (2.716×10^{-2})°	5.951×10^{-2} (2.714×10^{-2})*	5.998×10^{-2} (2.710×10^{-2})*
Diff. Retros-ref _D	4.596×10^{-3} (1.447×10^{-3})**			
Sum. Retros-ref _Σ	5.205×10^{-4} (6.572×10^{-4})			
Sum.Retros x Diff.Retros	-1.780×10^{-5} (6.799×10^{-6})**			
White.Retro		5.636×10^{-3} (2.696×10^{-3})°	1.223×10^{-3} (6.287×10^{-4})°	
Yellow.Retro		6.427×10^{-3} (4.950×10^{-3})***	-1.616×10^{-3} (1.255×10^{-3})	
W.Retro. x Y.Retro		-2.635×10^{-5} (1.563×10^{-5})***		
Segment ^a	3.700×10^{-1} (+0.332)	3.747×10^{-1} (+0.334)	3.795×10^{-1} (+0.335)	3.870×10^{-1} (+0.338)
Rt.Name ^a	9.306×10^{-2} (+0.166)	8.982×10^{-2} (+0.163)	9.096×10^{-2} (+0.164)	8.845×10^{-2} (+0.161)
Residual ^a	8.465×10^{-1}	8.503×10^{-1}	8.518×10^{-1}	8.505×10^{-1}
NB2	18.5108	18.1153	17.8559	17.6675
Number of data points	1955	1955	1955	1955
Number of segments	513	513	513	513
Number of Parameters	10	10	9	7
AIC	3344.167	3347.57	3348.29	3347.845
BIC	3399.948	3403.558	3398.498	3386.892
Log Likelihood	-1662.083	-1663.889	-1665.147	-1666.923
Chi-Sq.(deg. freedom)	9.680 (3)*	6.068 (3)	3.552 (2)	-
Significance values are as follows: ° p<0.1; * p < 0.05; ** p < 0.01; and *** p < 0.001				
Empty cell = not applicable				
^a Deviance of random effect. (Intraclass Correlation Coefficient)				

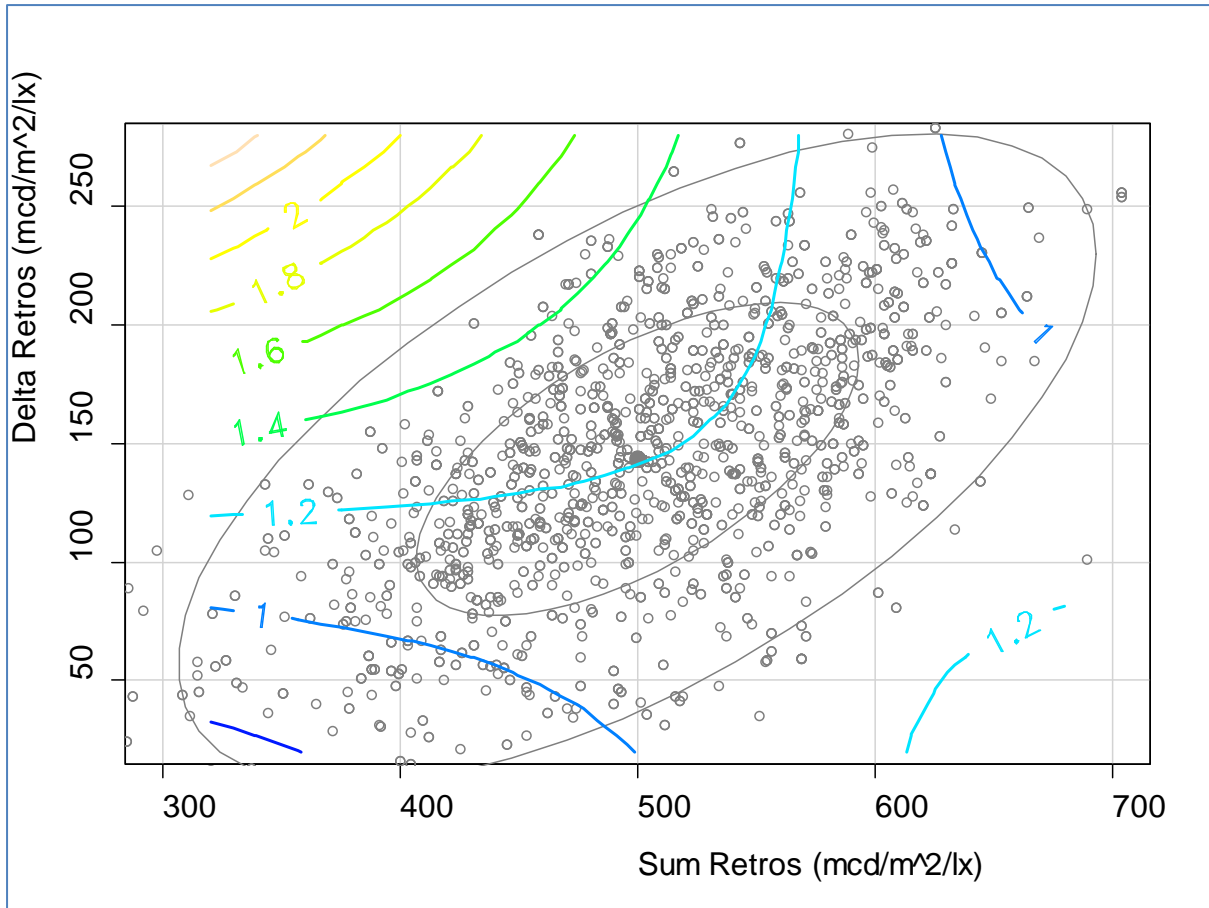


FIGURE 1 Contour plot for the safety factor of sum and delta of retroreflectivities of pavement markings.

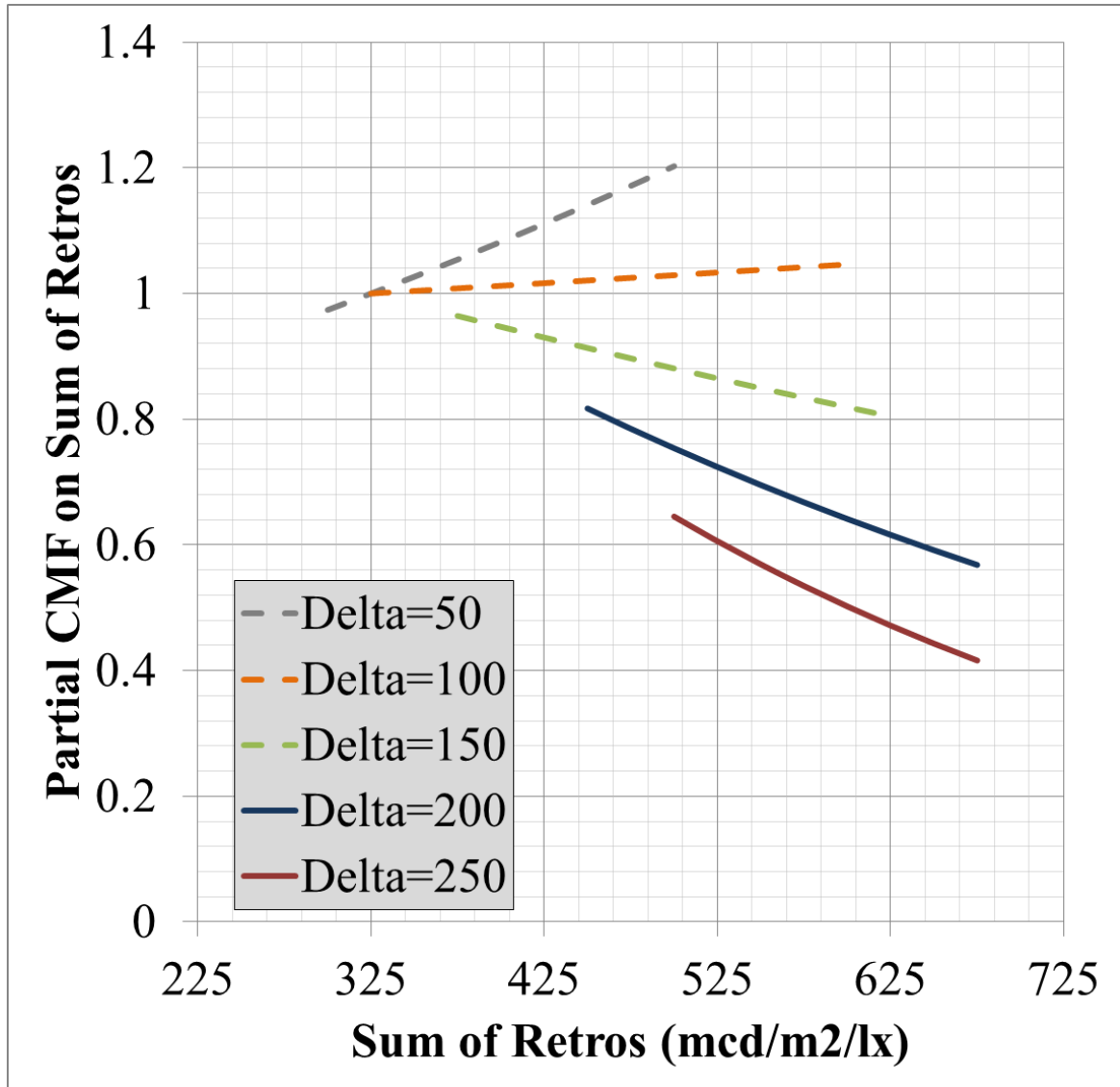


FIGURE 2 Marginal CMFs on the sum of retroreflectivities.

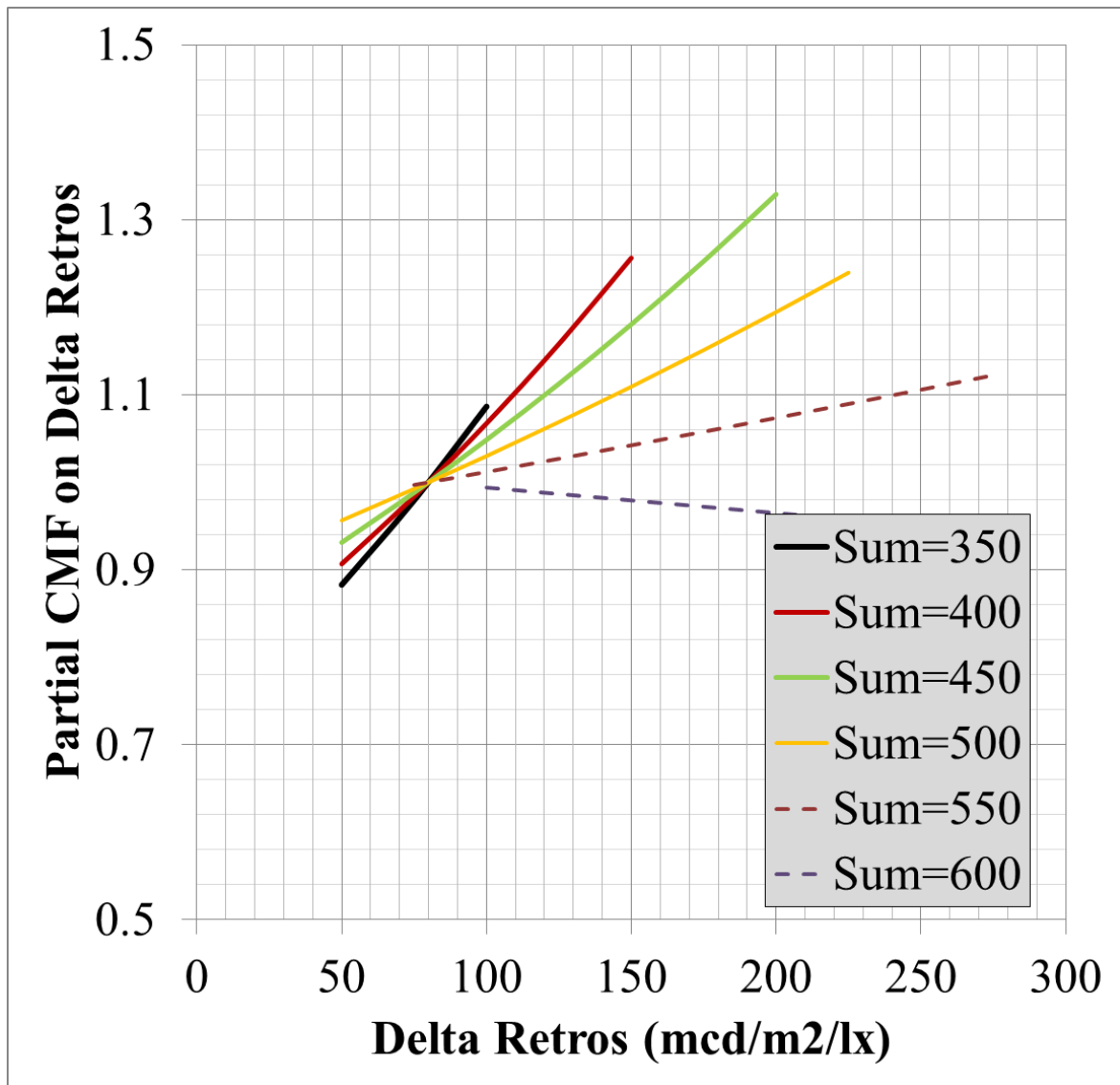


FIGURE 3 Marginal CMFs on the delta of retroreflectivities.

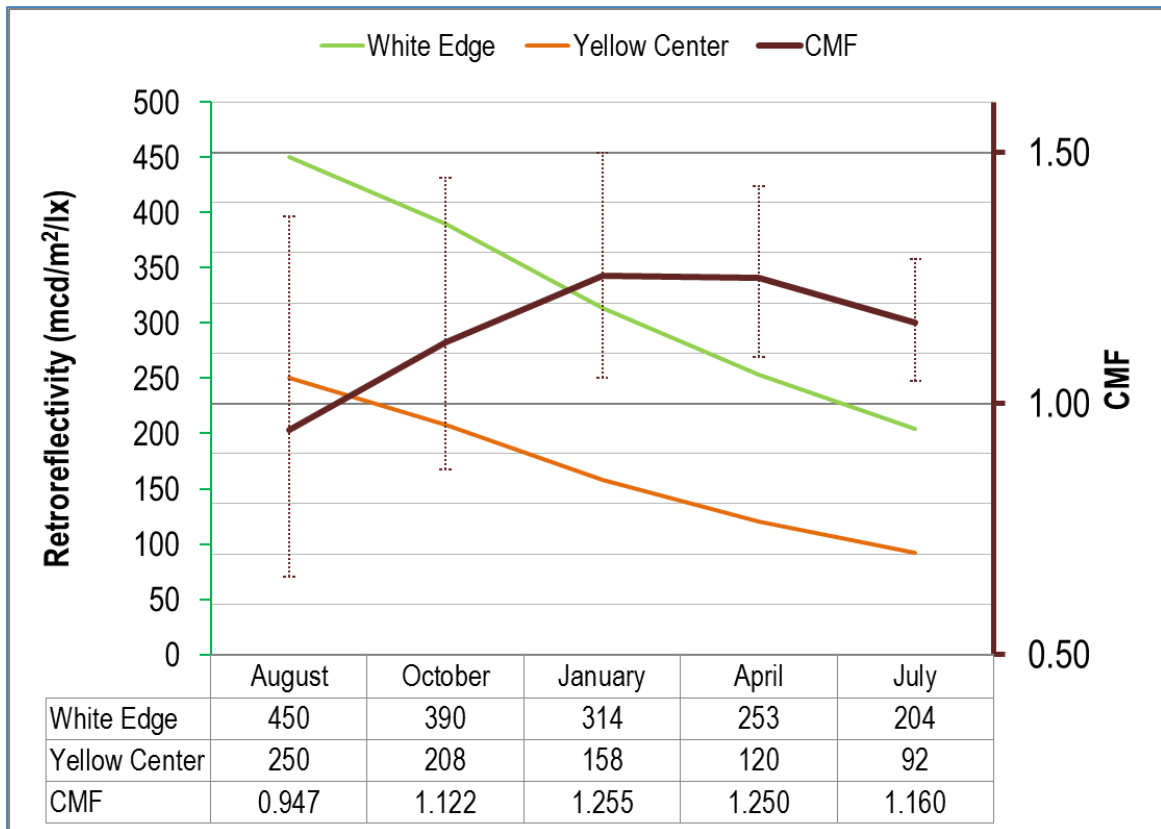


FIGURE 4 Yearly cycle trace of retroreflectivity and its safety factor for a hypothesized site.

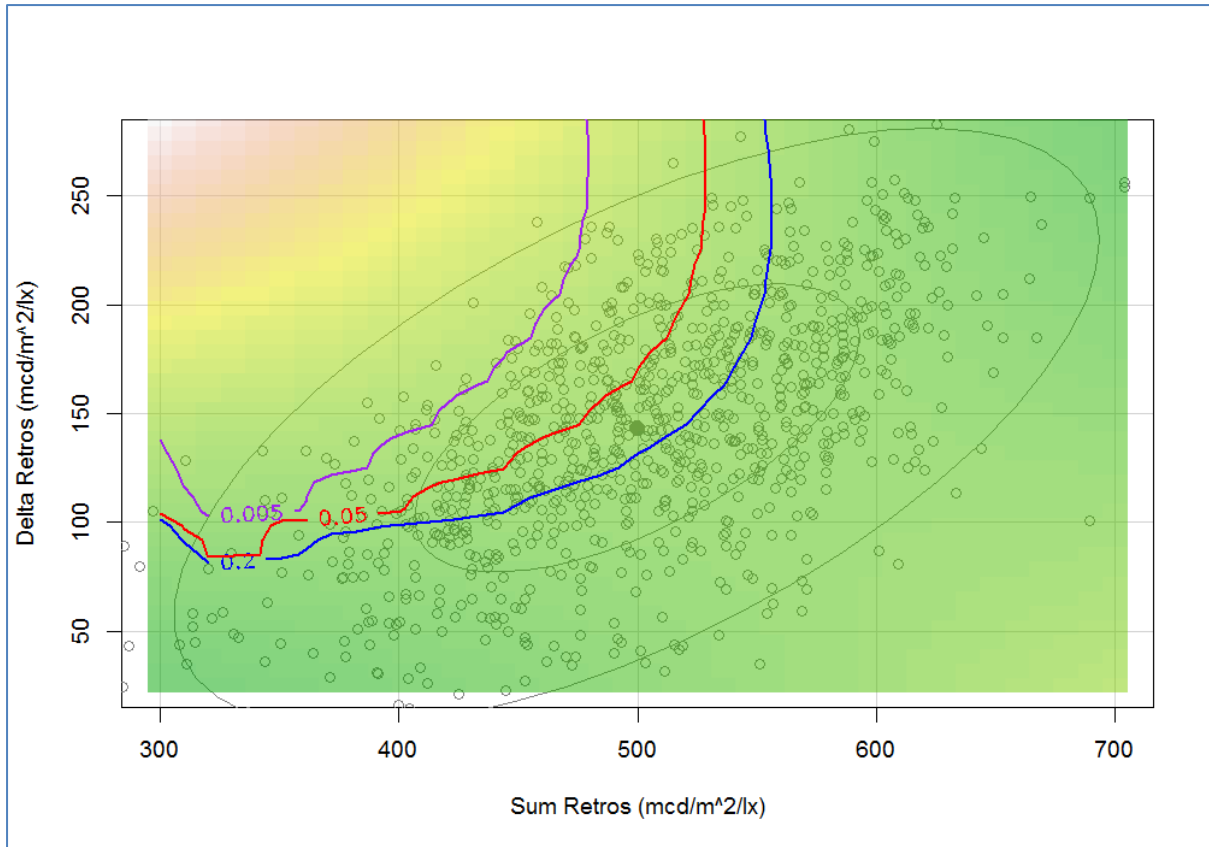


FIGURE 5 Statistical significance of Ho: CMF>1.0.

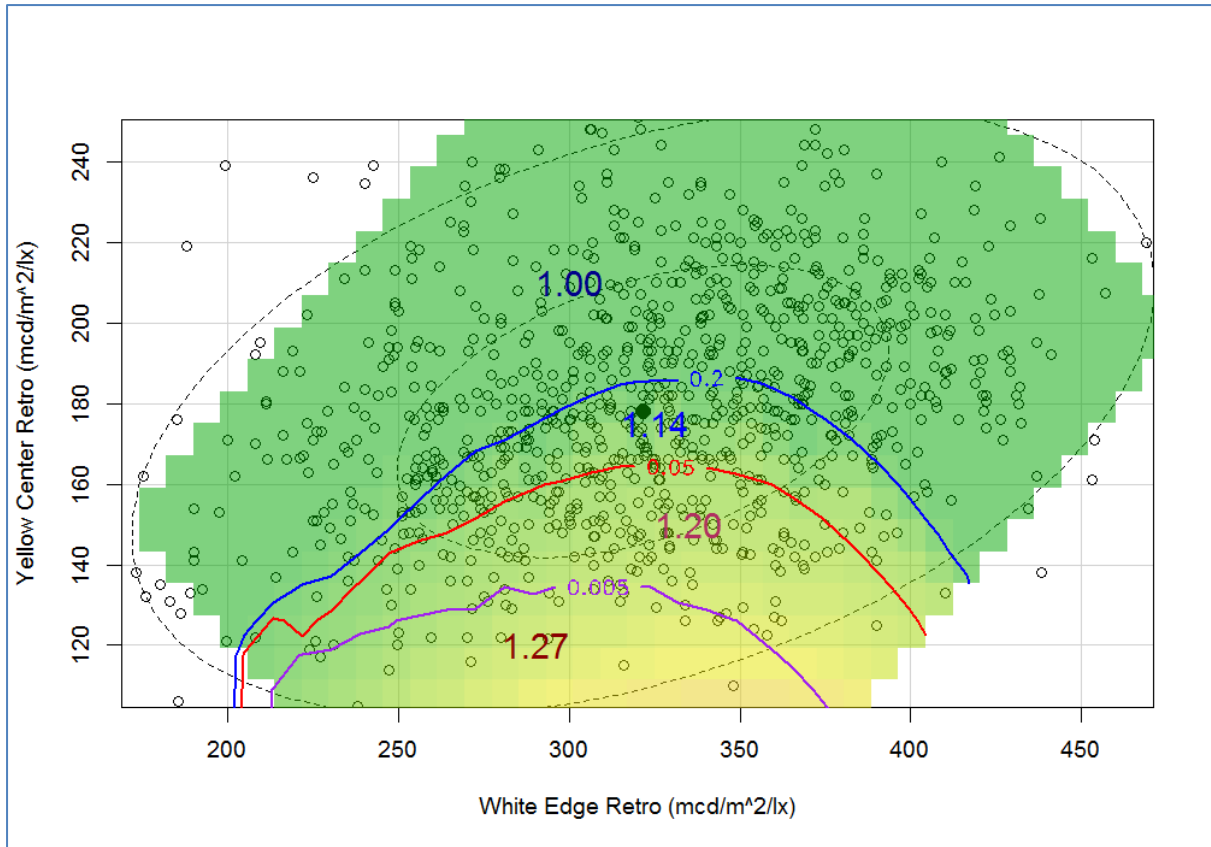


FIGURE 6 Average CMF by zone of Statistical Significance.